Article

Improved EfficientNet Architecture for Multi-Grade Brain Tumor Detection

Ahmad Ishaq [1,†] **, Fath U Min Ullah** [2,†] **, Prince Hamandawana** [3] **, Da-Jung Cho** [1] **and Tae-Sun Chung** [1,*]

1   Department of Artificial Intelligence, Ajou University, Suwon 16499, Republic of Korea;
    ahmadai@ajou.ac.kr (A.I.); dajungcho@ajou.ac.kr (D.-J.C.)
2   Department of Computing, School of Engineering and Computing, University of Central Lancashire,
    Preston PR1 2HE, UK; fath3797@gmail.com
3   Department of Software, Ajou University, Suwon 16499, Republic of Korea; phamandawana@ajou.ac.kr
*   Correspondence: tschung@ajou.ac.kr
†   These authors contributed equally to this work.

Abstract: Accurate detection and diagnosis of brain tumors at early stages is significant for effective treatment. While numerous methods have been developed for tumor detection and classification, several rely on traditional techniques, often resulting in suboptimal performance. In contrast, AI-based deep learning techniques have shown promising results, consistently achieving high accuracy across various tumor types while maintaining model interpretability. Inspired by these advancements, this paper introduces an improved variant of EfficientNet for multi-grade brain tumor detection and classification, addressing the gap between performance and explainability. Our approach extends the capabilities of EfficientNet to classify four tumor types: glioma, meningioma, pituitary tumor, and non-tumor. For enhanced explainability, we incorporate gradient-weighted class activation mapping (Grad-CAM) to improve model interpretability. The input MRI images undergo data augmentation before being passed through the feature extraction phase, where the underlying tumor patterns are learned. Our model achieves an average accuracy of 98.6%, surpassing other state-of-the-art methods on standard datasets while maintaining a substantially reduced parameter count. Furthermore, the explainable AI (XAI) analysis demonstrates the model's ability to focus on relevant tumor regions, enhancing its interpretability. This accurate and interpretable model for brain tumor classification has the potential to significantly aid clinical decision-making in neuro-oncology.

Keywords: medical imaging; brain cancer; medical informatics; deep learning; transfer learning; model tuning; image classification

1. Introduction

Brain tumors, particularly those originating in the central nervous system (CNS), represent a significant public health challenge due to their high mortality rates and the complexity of their diagnosis and treatment. Brain tumor detection is a critical task in medical imaging, as early and accurate diagnosis can significantly improve patient outcomes. However, brain tumors are highly diverse, with different types and grades that present unique challenges for accurate classification and timely intervention. According to the United States National Institute of Health (NIH), an estimated 25,400 new cases of brain and CNS cancers are expected in 2024, with 18,760 deaths projected in the same year [1]. Globally, the burden is even more pronounced, with 308,102 new cases and 251,329 deaths reported in 2020, as highlighted in the Global Cancer Statistics 2020 [2]. These alarming statistics

underscore the urgent need for advanced diagnostic tools and techniques to address the challenges posed by the heterogeneity of brain tumors and improve patient care.

Medical imaging modalities, such as X-rays, ultrasound, computed tomography (CT), and magnetic resonance imaging (MRI), play an indispensable role in the clinical diagnosis of brain tumors. These imaging techniques provide detailed information on the location, size, and characteristics of tumors, allowing clinicians to make informed decisions about treatment strategies. However, challenges such as the precision and timeliness of imaging-based diagnoses are highly dependent on the expertise of radiologists, which can lead to delays in diagnostic procedures. Such delays not only hinder surgical planning and additional treatments but also limit the enrollment of patients in clinical trials, further exacerbating the challenges in the management of this deadly disease [3,4]. In recent years, artificial intelligence (AI)-based techniques, particularly deep learning, have emerged as powerful tools to enhance the precision and efficiency of brain tumor diagnosis. Deep learning algorithms, which are capable of analyzing vast amounts of medical imaging data, have shown remarkable potential in automating the detection and classification of brain tumors. By leveraging these technologies, healthcare providers can bridge the gap in access to early diagnostic care, especially in resource-limited settings where the availability of skilled radiologists is limited. AI-driven systems can help identify tumors in earlier stages, thus facilitating timely interventions and improving patient outcomes [5–7]. Researchers have conducted extensive investigations using computer vision and artificial intelligence in clinical applications over the past decade through computer-aided diagnosis (CAD) systems [8]. The authors in [9] demonstrate AI's potential to improve brain tumor diagnosis and treatment, paving the way for personalized medicine and better patient outcomes. Fast-growing brain tumors require prompt treatment, which requires deep learning and CAD systems for tumor detection and feature extraction in early diagnosis. Recent advances in computing power through GPUs and TPUs have enabled the deep learning community to develop CNN architectures with enhanced accuracy and efficiency. These improvements drive the implementation of such models for the diagnosis of brain tumors. A comprehensive review by [10] examines various CNN architectures for processing medical images, particularly brain MRI scans. Despite CNN advancements, significant challenges remain in brain tumor detection, specifically in developing accurate classification techniques for various types and grades of tumors. Current AI methods are limited by small annotated datasets crucial for training robust models. The rarity of certain tumor types and high data collection costs result in models that struggle with generalization across patient populations and imaging modalities. Class imbalance poses another challenge, where underrepresented tumor types lead to biased models with poor performance in minority classes. Multi-grade tumor classification demands models that can distinguish subtle tumor characteristics. While deep learning models show promising accuracy, their black box nature limits insight into decision-making processes, hindering clinical adoption where explainability is essential for healthcare professional trust. Addressing these challenges requires innovative solutions such as advanced data augmentation, interpretable AI models, and diverse datasets to enhance the reliability of AI-driven brain tumor detection systems.

To tackle these challenges, our research focuses on the multi-classification of brain tumor types into four classes based on MRI data and on enhancing model interpretability through techniques like Grad-CAM. Many machine learning and deep learning algorithms are used in image classification, segmentation, and feature extraction [11,12]. We propose an improved variant of EfficientNet for multi-grade brain tumor classification. EfficientNet is a state-of-the-art CNN architecture with remarkable performance in various image classification tasks, including medical image analysis [13]. We chose EfficientNet due to its ability to scale up principally, allowing for an optimal balance among network depth,

width, and resolution [14]. Our proposed model improves EfficientNet's capabilities for four-grade classification (glioma, meningioma, pituitary, and non-tumor) and incorporates gradient-weighted class activation mapping (Grad-CAM) for enhanced interpretability. By integrating Grad-CAM, we address the gap between the performance and explainability in existing models, providing insights into the model's decision-making process and increasing trust in its predictions. Another investigation [15] encompasses three distinct methods employing various architectures of CNNs, including AlexNet, GoogLeNet, and VGGNet, for the classification of brain tumors. These studies adopt transfer learning techniques, specifically fine-tuning and weight freezing, leveraging MRI slices from the brain tumor dataset. However, it is important to note that data augmentation may not consistently enhance model efficiency unless the augmented data aligns closely with the original input distribution, avoiding significant shifts [16]. Therefore, it is imperative to ensure that the chosen data augmentation strategies are consistent and genuinely contribute to improving model accuracy.

Motivated by this insight, we employ three distinct datasets to assess our model's performance. The first dataset [17] is relatively small, prompting the use of data augmentation to optimize model accuracy. Conversely, the second dataset [18] is larger in scale and does not undergo any data augmentation. This approach allows us to evaluate our model's consistency in brain tumor classification across both smaller and larger datasets, ensuring robust performance across varying data sizes. Our study aims to enhance deep learning models for multi-grade brain tumor classification by improving accuracy, interpretability, and parameter efficiency. Our key contributions are as follows:

- We, for the first time, extend and improve an enhanced version of the EfficientNet model tailored for multi-grade brain tumor classification, marking the first implementation of this enhanced architecture for classifying four distinct tumor classes, expanding from traditional three-grade to four-grade classification while maintaining the capability to extend to multiple classification heads.
- We analyze and evaluate the efficiency of the enhanced model across datasets of varying sizes, aiming to ensure classification consistency. Our evaluations show the superior performance of the improved model compared to the state-of-the-art EfficientNet models. Our findings, validated through diverse performance metrics, demonstrate the superior performance of our model compared to the already proven state-of-the-art EfficientNet models.
- For explainable artificial intelligence (XAI), the Grad-CAM visualization is incorporated to enhance the model's interpretability. This technique provides valuable insights into the model's decision-making process by highlighting the regions of MRI images most influential in tumor classification, thereby increasing the model's transparency and potential for clinical application.

The remainder of this paper is organized as follows: Section 2 focuses on some related literature. In Section 3, the proposed model is presented in detail, covering preprocessing, data augmentation, and transfer learning techniques used in our approach, while Section 4 presents the results of the experiments conducted. Section 5 provides the conclusions and summarizes our work, and lastly, Section 6 discusses the limitations and future directions of our research.

2. Literature Review

2.1. Conventional Image Analysis with ML

Over a decade, numerous studies have explored the application of machine learning (ML) techniques in medical image analysis, particularly for brain tumor detection. Early research focused on conventional ML methods such as support vector machine (SVM),

k-nearest neighbors (KNNs), and random forest classifiers, as well as hybrid approaches combining KNN and artificial neural networks [19]. However, the emergence of sophisticated deep learning architectures, especially convolutional neural networks (CNNs), has revolutionized the field [20]. Several variants of CNN came into practice; for instance, [21] employed ResNet [22], GoogLeNet's Xception network [23], and MobileNet-V2 [24] to classify brain tumors into two classes, demonstrating the effectiveness of state-of-the-art CNN architectures in enhancing accuracy and efficiency in brain tumor medical image analysis. A comprehensive study [25] conducted an extensive investigation into various diagnostic enhancement techniques for brain MRI images, examining deep learning, transfer learning, and classification methodologies, and elaborating on their respective advantages, limitations, developments, and future trends. These advancements have paved the way for further exploration and refinement of DL techniques in the domain of AI-based computer-aided diagnosis systems for brain tumor detection.

2.2. Key CNN Models for Medical Image Analysis

Aiming to optimize the performance for specific problem domains, researchers frequently experiment with various neural network architectures. A comparative analysis in prior work [26] involving deep neural networks (DNNs) and convolutional neural networks demonstrates that ResNet-50 exhibits notable performance in brain tumor classification, employing transfer learning techniques to discern tumor types such as glioma, meningioma, and pituitary tumors. As computer vision witnesses the emergence of numerous convolutional neural network architectures, researchers explore their applicability across diverse tasks. Each model has distinct advantages and limitations: VGG [27] proves advantageous with small datasets and constrained computational resources, while ResNet [22] is preferred with extensive datasets and ample computational capabilities. However, enhancing ResNet's accuracy by scaling layers increases computational complexity and training durations, and may overfit with scarce datasets. Seeking a balance between computational efficiency and accuracy, Google introduced EfficientNet [14], surpassing other CNN architectures in top-1 accuracy on ImageNet and establishing new transfer learning benchmarks. In brain tumor classification, EfficientNet-B0 [28] was tailored for binary classification, distinguishing normal brain scans from benign tumors, while EfficientNet-B7 [13] was designed for multi-grade classification, extending the framework to classify three tumor types. Our study aims to enhance the effectiveness of EfficientNet, which outperforms other state-of-the-art models (Table 1), by optimizing accuracy and training efficiency for more than three grades of brain cancer. We introduce new layers to the base EfficientNet-B7 model (Section 3), making it extendable to more than four multi-class classification heads, thus creating a versatile and powerful tool for brain tumor classification tasks.

Table 1. Summary of previously discussed research works with their proposed methodology.

Method	Accuracy	Classification (Size)	Dataset
Multi-Scale CNN (MSCNN) [29]	91.2%	Multi-class (4)	Kaggle
Pre-trained VGG-19 [30]	90.67	Multi-class (4)	Radiopaedia/Brain tumor
ResNet, Xception, and MobilNet-V2 [21]	95%, 97.35%, 98.24%	Binary	kaggle
EfficientNet-B0 [28]	98.87%	Binary	Kaggle
EfficientNet-B7 [13]	98.86%	Multi-class (3)	Figshare

2.3. Vision Transformers for Image Processing

CNNs have long been the dominant architecture for medical image analysis. However, vision Transformers (ViTs), introduced by [31], have emerged as a promising alternative. Unlike CNNs, which rely on local feature extraction, ViTs use self-attention mechanisms

to model long-range dependencies in images, making them particularly suitable for complex tasks, such as brain tumor classification and segmentation [32]. These models are increasingly being integrated with CNN architectures in hybrid models to improve classification performance. By combining the local feature extraction capabilities of CNNs with the global contextual understanding of ViTs, researchers aim to enhance tumor classification accuracy, ultimately aiding in more precise diagnosis and personalized treatment strategies [33]. However, a key limitation of ViTs is their reliance on large-scale datasets for effective training. Unlike CNNs, which have built-in inductive biases for local structure learning, ViTs require substantial labeled data to learn meaningful representations. Ref. [31] highlight that when ViTs are trained on small datasets without extensive pre-training or strong regularization, they tend to overfit and perform worse than CNNs. Due to this reason, we adopt CNNs for better classification, as they work better on smaller amounts of data.

3. Proposed Method

This section sheds light on the proposed approach for brain tumor classification utilizing MRI images. Our parameter-efficient convolutional neural network draws inspiration from the scalable EfficientNet-B7 model [13]. The detailed working flow of the proposed framework for the method is depicted in Figure 1. To refine the baseline EfficientNet-B7 ConvNet, our initial step involves preprocessing the images belonging to the four classes of brain tumors. This preprocessing stage encompasses dividing the dataset into training, testing, and validation sets. Given the heterogeneous sizes of MRI images within the dataset, we standardize their dimensions through resizing. Additionally, within the preprocessing module, we employ several data augmentation techniques, detailed in Section 3.1, aimed at mitigating the challenge of limited data. These techniques augment the input data size by applying diverse transformations to the existing images. The augmented images that have undergone processing and transformations are utilized as input for the EfficientNet-B7 model, which forms the foundation of our enhanced model. To further mitigate the impact of limited datasets, we incorporate transfer learning techniques into the baseline EfficientNet-B7 model. This entails leveraging the pre-trained model's weights and parameters from the ImageNet dataset and adapting them to our specific brain tumor classification task using our proposed enhanced model. Through this process, the weights of the pre-trained model are fine-tuned with the additional layers to optimize performance for the brain tumor classification task. These refined weights are then employed in classification tasks, empowering the model to generate informed and accurate predictions. A comprehensive explanation of each step within the proposed methodology is provided in subsequent sections.
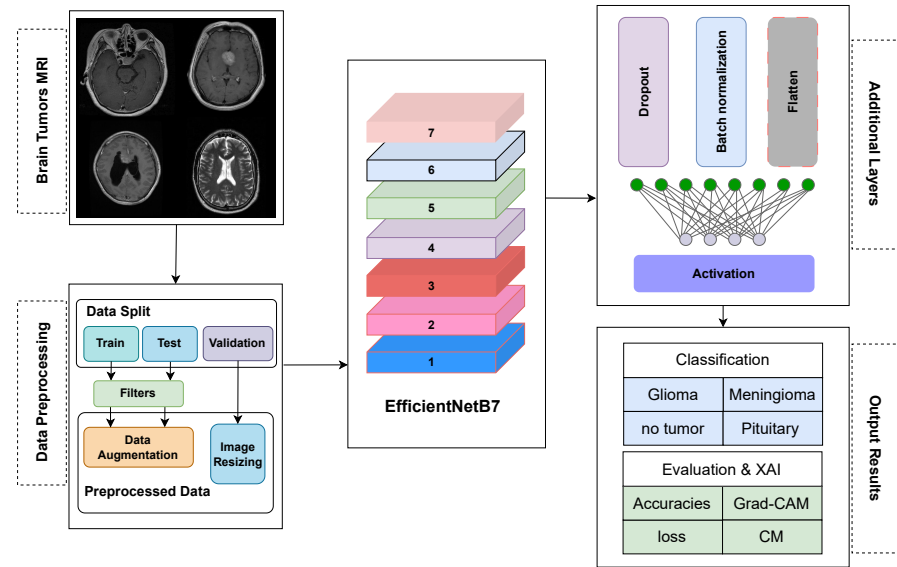
Figure 1. Overview of the proposed model framework where the pre-processed MRI input data, obtained through data splitting, filtering, augmentation, and resizing, is fed into the feature extraction network. Based on the features, the trained model classifies the input images as glioma, meningioma, pituitary tumor, or non-tumor categories. Input image sample taken from the BT-3264 dataset [17].

3.1. Preprocessing

The preprocessing stage is fundamental in obtaining image data for utilization within deep learning models, ensuring optimal performance during the training and validation phases. Leveraging the Keras library [34], we utilize the apply filters function to execute a series of image transformations before their integration into the training or testing pipeline. Initially, a Gaussian blur filter with a sigma value of $\sigma = 1.5$ is applied to the images. This filter operates by convolving the image with a Gaussian function, where Sigma (σ) determines the extent of blurring. A large Sigma value impacts the blurring, while a smaller value preserves the fine information. By mitigating noise, the filter facilitates a cleaner representation of image content, thereby optimizing subsequent feature extraction processes.

Following the Gaussian blur, a sharpening filter with a minimum lightness factor of 1.5 is applied. This filter is instrumental in accentuating edges and fine details present within the image. By enhancing these features, the filter contributes to the preservation of critical image characteristics, ultimately aiding in the discernment of intricate patterns during model training. In addition to the Gaussian blur and sharpening filters, an edge detection filter with an alpha value of $\alpha = 1.0$ is applied. This filter effectively highlights the edges and contours inherent within the images, further refining the delineation of key features. By emphasizing these structural elements, the filter enhances the discriminative capabilities of the model, facilitating the extraction of meaningful information crucial for accurate classification. Collectively, these filters applied within our preprocessing module serve to enhance the saliency of features present within the images. By optimizing image clarity and accentuating critical details, the preprocessing stage ensures that the neural network can effectively extract and learn meaningful patterns during the subsequent training process, thereby enhancing the overall efficacy of the classification model.

Data augmentation is a fundamental technique pivotal to expanding the diversity inherent within the training dataset and assisting the model's resilience against variations encountered in the input data. In our implementation, we apply two separate image data generator objects: one dedicated to training data and the other tailored for testing

data. These generators act as a pipeline for executing a comprehensive suite of data augmentation procedures, thereby enriching the variability encapsulated within the dataset. To maintain a coherent joint distribution between the original data and its augmented counterparts, we carefully adhere to well-established augmentation techniques [16]. Within our methodology, we deliberately incorporate a mixture of fundamental and yet proven augmentation transformations shown in Figure 2. These transformations encompass a spectrum of operations, including horizontal and vertical flips, rotations spanning up to 90 degrees, and shearing with a factor of 0.2. Such operations hold particular relevance in scenarios, where objects within images manifest diverse perspectives or orientations. By introducing these transformations in a randomized fashion during the training phase, the model is systematically exposed to a broader spectrum of image variations. This strategic exposure not only fosters the model's adaptability but also fortifies its capacity for generalization across unseen data instances. This augmentation strategy profoundly enhances the model's ability to discern and extract meaningful features from the dataset.

The final harmonization of the preprocessing techniques and data augmentation strategies significantly amplifies the model's efficiency in distilling essential patterns from the dataset. This comprehensive approach not only improves the model's predictive performance but also furnishes it with the adaptability essential for navigating diverse real-world applications with high effectiveness and accuracy.
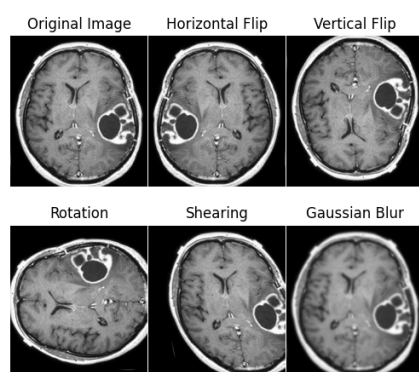

Figure 2. Tools applied to augment the MRI images. Input image sample taken from the BT-3264 dataset [17].

3.2. Improved Model and Its Parameters

Deep learning, especially convolutional neural network (CNN), excels in image analysis but requires large annotated datasets to avoid overfitting, a challenge in fields like medical imaging due to limited and sensitive data. Transfer learning addresses this by using knowledge from pre-trained models on large datasets like ImageNet and adapting it to smaller, specific datasets through fine-tuning. This approach is particularly useful in medical image analysis, such as brain tumor classification. In our solution, we explore the fine-tuning of the baseline model in a twofold approach. Firstly, we only perform fine-tuning on the baseline EfficientNet architecture without introducing any supplementary layers. Specifically, to align the baseline EfficientNet model with our method, we made alterations to the output layer and attached an additional classification head. This process entails refining the pre-existing baseline model and tailoring it to our specific task. The preprocessed data are passed as input to the EfficientNet layers, followed by flattening and forwarding to the output layer for final classification. We use this modified architecture as a standard to evaluate against our proposed approach. Secondly, we modify the baseline model and fine-tune it with additional layers. We incorporate these supplementary layers to capture more intricate features of the input images, thereby facilitating the discrimination among the four grades of tumors. The alteration leads to a modified architecture

characterized by three principal layer blocks, as depicted in Figure 1. The initial block inherits the seven layers from the baseline EfficientNet-B7 model. The second block adds fine-tuned layers with dropout and batch normalization for training stability. Finally, the third block includes a fully connected layer, flattening layer, ReLU activation, and a softmax output layer for multi-class classification of four brain tumors. To enhance the performance of the model when confronted with limited datasets, we leverage the strategy of transfer learning, coupled with fine-tuning the parameters and weights of the pre-trained baseline EfficientNet-B7 model, as depicted in Figure 3. This fine-tuning approach stands as an important method for training networks with constrained datasets. It involves utilizing the weights of a pre-trained model, initially trained on a large dataset, as the starting point, subsequently employing smaller datasets to update and refine these weights during training. Extensive empirical evidence supports the efficacy of this method in accomplishing various classification tasks effectively. Detailed descriptions of the added fine-tuning layers of the modified architecture are provided in Section 3.3.
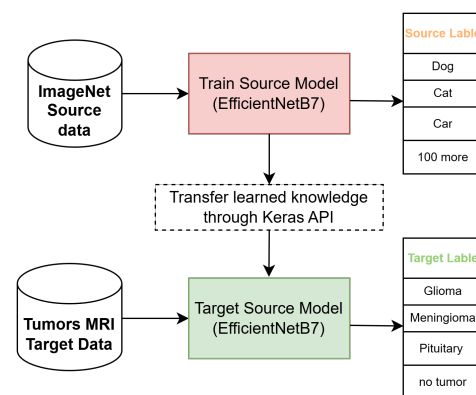

Figure 3. Adopted transfer learning method.

3.3. Layer Adjustment and Impact

In our effort to refine the neural network architecture dedicated to brain tumor classification, we carefully modify the EfficientNet-B7 model by incorporating additional layers aimed at fortifying its capabilities. These additional layers comprise a dropout layer, batch normalization layer, flattening layer, fully connected layer, and a ReLU activation layer, as depicted in Figure 1 as additional block layers. The introduction of the dropout layer serves a critical purpose: to mitigate the risk of overfitting by preventing the model from fixating excessively on the training data. By randomly disregarding segments of the data during training, this layer fosters a more generalized understanding of the input features, ensuring that the model does not become overly reliant on specific data points or patterns. To adapt the pre-trained EfficientNet-B7 model effectively and address the challenge of overfitting posed by limited tumor data, we adopted a strategic approach. This involved selectively freezing the layers within the initial block (Baseline EfficientNet-B7 layers) before introducing the dropout layer. This decision serves multiple key objectives: (i) preserving the network's capacity to generalize by averting over-reliance on specific features, (ii) mitigating the risk of overfitting, thereby ensuring the model's robustness to unseen data, and (iii) enhancing the network's capability to discern task-specific features pertinent to brain tumor classification. Subsequently, we integrate a batch normalization layer into the architecture to stabilize the training process by standardizing the input of preceding layers. This normalization mechanism alleviates issues associated with internal covariate shifts, thereby enhancing training stability and promoting improved generalization in the model. Additionally, a flattening layer is introduced to prepare the data for further processing. This involves reshaping the multi-dimensional output from the

batch normalization layer into a one-dimensional tensor, facilitating a seamless transition to subsequent layers.

To effectively capture the intricate patterns and relationships inherent in brain MRI images, a dense fully connected layer is introduced following the dropout, batch normalization, and flattening layers. This layer enables the network to contribute to learning the complex input data representations, thereby enhancing its discriminatory capabilities and enabling it to extract higher-level features relevant to tumor classification. Following the dense layer, a ReLU activation layer is incorporated to introduce non-linearity into the model. This activation function ensures that the model can capture non-linear relationships within the data more effectively, further enhancing its capacity to discern subtle patterns and variations. In the final layers, four classification heads are appended to facilitate the classification of four distinct classes of brain tumors. The model learns to assign probabilities to each class using a softmax activation function, facilitating effective multi-class classification. This softmax activation function transforms the model's raw output into probability distributions over the different classes, enabling informed decisions regarding the presence and severity of various types of brain tumors based on the model's predictions. Our model has the flexibility to expand to accommodate multiple classification heads in case of additional classes.

4. Experiments

This section presents our experimental results and analysis. To ensure reproducibility, we first detail our experimental environment setup in Table 2, which outlines the software framework and hardware specifications used in our implementation. Our experiments were conducted using the specified computational resources that provided sufficient capacity for our deep learning workload. We evaluated model performance through comprehensive metrics: accuracy, loss, precision, recall, AUC, and F1 score across different brain tumor classes. A confusion matrix demonstrates the model's classification performance for each tumor type. Additionally, we provide explainable AI (XAI) visualizations to illustrate the model's feature learning process. Finally, we compare our model's efficiency against existing approaches through a detailed parameter analysis.

Table 2. Software environment and system specifications.

Name	Specification
Software Environment	
Framework	TensorFlow 2.14
Base Image	NVIDIA NGC
Development	Python 3.10
Cloud Services	KT Cloud (NIPA)
Hardware Specifications	
GPU	NVIDIA V100Q
CPU Allocation	18 cores
System Memory	64 GB

4.1. Dataset

The experiments were conducted by utilizing three datasets in which two were sourced from Kaggle, namely BT-3264 [17] and BT-7023 [18], which encompass four distinct categories of brain tumors: glioma, meningioma, pituitary, and non-tumor class. The other dataset is from Figshare [35] with four classes, including glioma, meningioma, pituitary, and non-tumor. The distribution of the datasets across classes is reflected in detail in Table 3. The BT-3264 dataset is a bit smaller than the others. It has 3264 images, with 926 images of gliomas, 937 images of meningiomas, 901 images of the pituitary gland, and 500 images of

normal brain tissue. On the other hand, the BT-7023 dataset is more than twice the size, containing a total of 1621 glioma, 1645 meningioma, 2000 pituitary, and 1757 non-tumor images. Given the smaller image count of the BT-3264 dataset compared to BT-7024, there exists a risk of overfitting and diminished generalization. To mitigate this issue effectively, we implemented augmentation techniques on the BT-3264 dataset, thereby increasing the number of images and enhancing the model's learning capacity. To facilitate the analysis, we partitioned the datasets into separate sets for training and validation purposes. To confirm the consistency of our model, we also used the Figshare datasets. The Figshare dataset distribution consists of 1426 glioma, 708 meningioma, and 930 pituitary images.

Table 3. Distribution of dataset samples across brain tumor classes.

Tumor Types	BT-3264 Dataset Distribution			BT-7023 Dataset Distribution			Figshare Dataset Distribution		
	Training	Testing	Total	Training	Testing	Total	Training	Testing	Total
Glioma	826	100	926	300	1321	1621	1141	285	1426
Meningioma	822	115	937	306	1339	1645	566	142	708
Pituitary	827	74	901	405	1595	2000	744	186	930
Non-Tumor	395	105	500	300	1457	1757	–	–	–
			3264			**7023**			**3064**

4.2. Performance Evaluation

The information in this section provides a full breakdown of the outcomes of training and validating our suggested model, which is meant to correctly label MRI images showing brain tumors. We leveraged three distinct datasets, namely BT-3264, BT-7023, and Figshare, aiming to provide an understanding of the model's performance across varying data sizes and complexities. The decision to utilize three datasets stems from their primary considerations:

- In light of the scarcity of available brain tumor images, it becomes imperative to evaluate the robustness and adaptability of our model under real-world scenarios, particularly when dealing with smaller datasets. To confront this challenge head-on, we implement data augmentation techniques, as outlined in Section 3.1, specifically tailored to enhance the efficacy of the smaller BT-3264 dataset.
- Additionally, it is crucial to gauge the scalability and consistency of our model when confronted with considerably larger datasets. Therefore, we conduct an expanded evaluation using the larger BT-7023 dataset, opting not to employ any augmentation techniques, thus ensuring a direct comparison under varying data scales.
- In light of the diverse and complex nature of brain tumor imaging data, it is essential to assess the robustness and generalization of our model across datasets of varying scales and characteristics. To address this, we leverage the Figshare dataset, which is widely recognized and utilized in brain tumor research for its comprehensive collection of multi-modal MRI scans.

Building upon the findings presented in Section 2 and the comprehensive analysis detailed in Table 1, our study underscores the superior performance exhibited by the EfficientNet-B7 model when compared against other state-of-the-art models, including Multi-Scale CNN, VGG-19, ResNet, Xception, and MobileNet-V2, in the area of multi-class brain tumor classification tasks.

Primary objective of evaluation: The primary objective in this investigation is to conduct a comparative assessment between our proposed brain tumor classification model and the established state-of-the-art EfficientNet-B7 model. In all experiments, we refer to

the EfficientNet-B7 model and our proposed model as the baseline and customized model, respectively.

4.2.1. Evaluation Using Smaller BT-3264 Dataset

To validate and assess the effectiveness of our proposed model on datasets with limited sample sizes, we conducted an evaluation focusing on the accuracy and loss performance using the BT_3264 dataset. Data augmentation was applied to both the baseline and our customized model. Illustrated in Figure 4, the comparative analysis presents the curves of loss and accuracy throughout the training process for both the baseline and customized models.

(**a**) Baseline Accuracy

(**b**) Customized Model Accuracy

(**c**) Baseline Model Loss

(**d**) Customized Model Loss
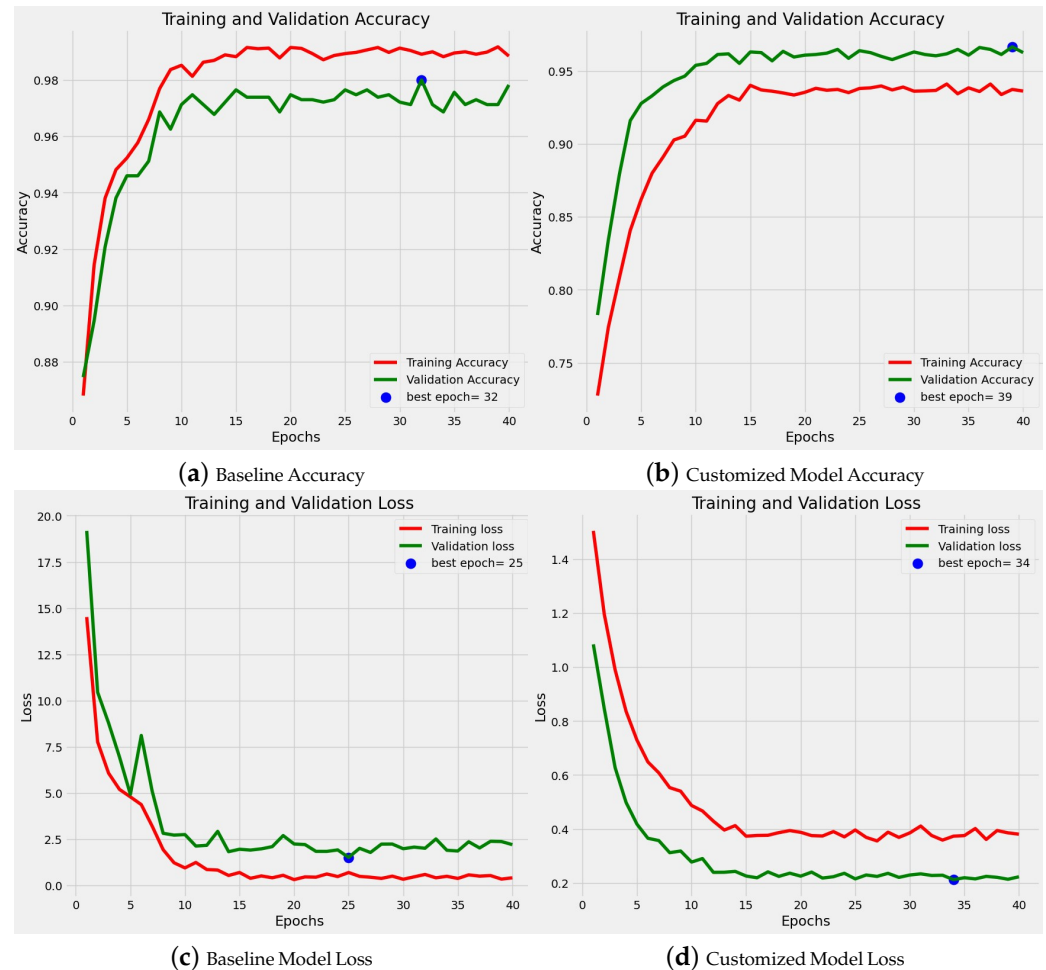
Figure 4. Accuracy and loss comparison between baseline and customized approach using small dataset BT_3264.

In Figure 4a,c, experimental results for the baseline model are depicted. Here, we observe fluctuating patterns in both loss and accuracy curves, indicating inherent instability. Although training accuracy consistently surpasses validation accuracy, occasional reversals are observed across epochs. The baseline model starts with lower training loss but converges with validation loss around epoch 25, identified as a critical point of optimal performance. Beyond epoch 25, validation loss slightly exceeds training loss, suggesting potential challenges in generalization on smaller workloads. These findings underscore the necessity for model refinement or incorporation of regularization techniques to enhance stability and generalization on the baseline model.

In contrast, Figure 4b,d illustrate the performance of our customized model, engineered with specific adjustments to enhance stability. Notably, training accuracy starts

from a lower point compared to validation accuracy and consistently lags throughout, with validation accuracy consistently outperforming training accuracy. The optimal epoch, identified at 39, signifies the divergence point of our customized model. Furthermore, while training loss initiates at a higher value compared to validation loss, validation loss consistently remains below training loss post-divergence of our customized model. This significant improvement in generalization indicates the model's enhanced performance on unseen data compared to the baseline model. These enhancements are attributed to the additional optimization layers detailed in Sections 3.2 and 3.3.

Despite achieving optimal convergence at the start, the baseline model encounters challenges in stability and generalization, contrasting with the customized model, which incorporates deliberate adjustments for augmented stability and improved accuracy and loss metrics. Quantitatively, the baseline model demonstrates a divergence point with validation accuracy at 95% and loss at 2%, indicating inferior performance compared to our customized model, which shows a validation accuracy of 97% and loss of 0.3%. This comprehensive analysis underscores the significance of tailored adjustments in optimizing model performance, even in the context of smaller dataset sizes.

4.2.2. Evaluation Using Larger BT-7023 Dataset

To assess the scalability and consistency of our model when dealing with considerably larger datasets, we employed the BT-7023 dataset. Given its larger image count, augmentation techniques were not applied to this dataset. Both our customized model and the baseline EfficientNet-B7 were evaluated for performance. Figure 5a,c display the accuracy and loss results for the baseline model, while Figure 5b,d illustrate the accuracy and loss outcomes of our customized model.

In Figure 5b, we observe that the training accuracy of the customized model starts at 80%, while the validation accuracy commences higher at around 90%. Throughout the training process, both curves exhibit similar growth patterns, closely aligning with each other. Towards the end, the validation accuracy stabilizes at 98%, slightly surpassing the training accuracy, which stabilizes at 97%. The optimal epoch is determined to be seven for the customized model. Notably, the customized model trained with the larger BT-7023 dataset demonstrates increased stability in model training. Turning to the loss results of the customized model depicted in Figure 5d, we observe a similar trend in training stability, where the training and validation curves converge towards each other. At the convergence point, the validation loss significantly outperforms the training loss, indicating consistent generalization of the customized model even with larger datasets. In contrast, as observed in Figure 5a, the baseline model exhibits rapid convergence in both training and validation curves, suggesting a potential case of overfitting. This underscores the necessity for the additional fine-tuning and customization proposed in Sections 3.2 and 3.3 to mitigate overfitting and enhance model performance. In summary, while the baseline model shows rapid convergence and fluctuations, indicating potential challenges with overfitting, the customized model with adjustments, achieves a balanced performance and demonstrates better generalization. These findings highlight the critical importance of tailored adjustments and careful consideration of model complexity in optimizing brain tumor classification models for clinical applications. In Figure 6, we present the confusion matrix obtained from our brain tumor classification evaluation using the extensive BT-7023 dataset. Since we have already shown consistency in the performance of our customized model, we forego presenting the confusion matrix for the smaller dataset at this point, as the results from the large dataset are deemed sufficient. Analysis of the confusion matrix reveals significant overfitting in the baseline model, collaborating with the 100% training accuracy shown in Figure 5a. However, the baseline model's inability to generalize

effectively is apparent in the mis-classifications exhibited within the confusion matrix. To mitigate this issue, recommendations include the implementation of robust regularization techniques and the exploration of a more fine-tuned model, as highlighted in our proposed model. Conversely, our customized model's confusion matrix showcases fewer instances of misclassification compared to the baseline model, highlighting its improved generalization capabilities for optimal brain tumor classification.
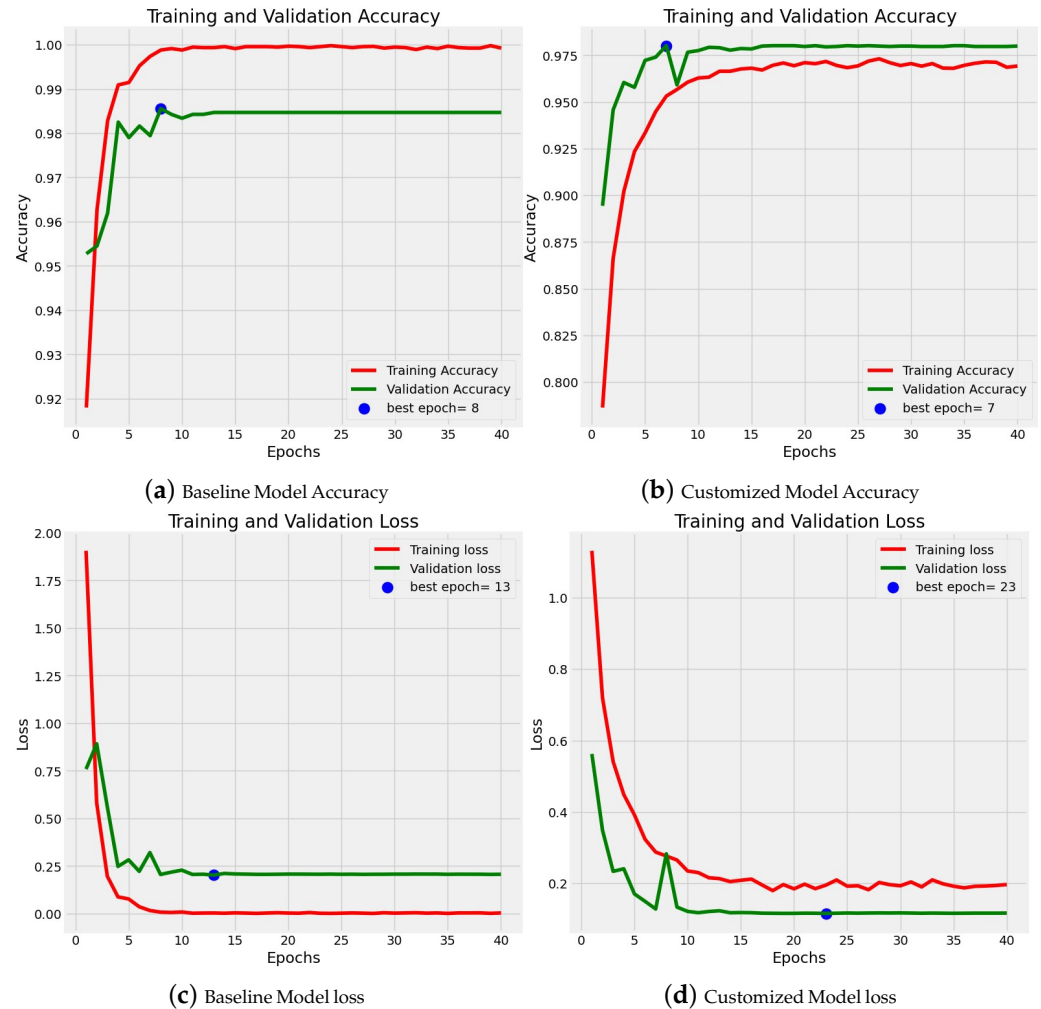

(**a**) Baseline Model Accuracy

(**b**) Customized Model Accuracy

(**c**) Baseline Model loss

(**d**) Customized Model loss

Figure 5. Accuracy and loss comparison between baseline and customized mode using larger dataset BT_7023.

Figure 7 presents comparative results on the Figshare dataset, reinforcing findings from our previous experiments. In Figure 7, the customized model demonstrates robust performance with training and validation metrics converging harmoniously. Both accuracy curves stabilize around 0.95, while the loss curves show consistent convergence after epoch 20, indicating strong generalization capability. In contrast, the figure reveals overfitting tendencies in the baseline model despite rapid initial convergence. While training accuracy approaches 1.0 and loss nears 0, the validation metrics diverge significantly, with accuracy plateauing at 0.96 and loss stabilizing around 0.3. This performance gap between training and validation metrics suggests that the baseline model compromises generalization by overfitting to the training data, whereas our customized approach successfully mitigates this limitation.
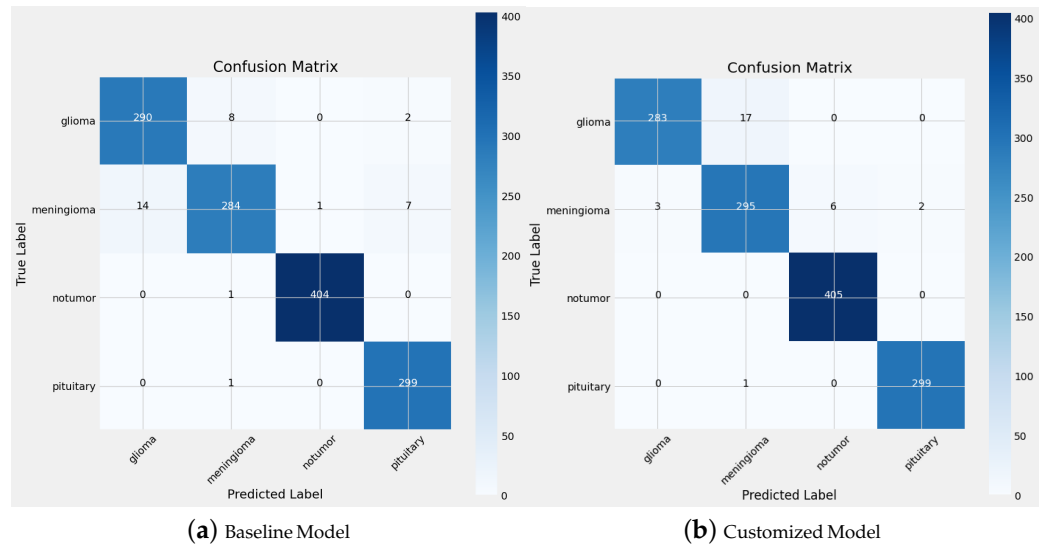
(**a**) Baseline Model

(**b**) Customized Model

Figure 6. Confusion matrix of BT_7023 with baseline and customized model.

(**a**) Customized Model loss

(**b**) Customized Model Accuracy

(**c**) Baseline Model loss
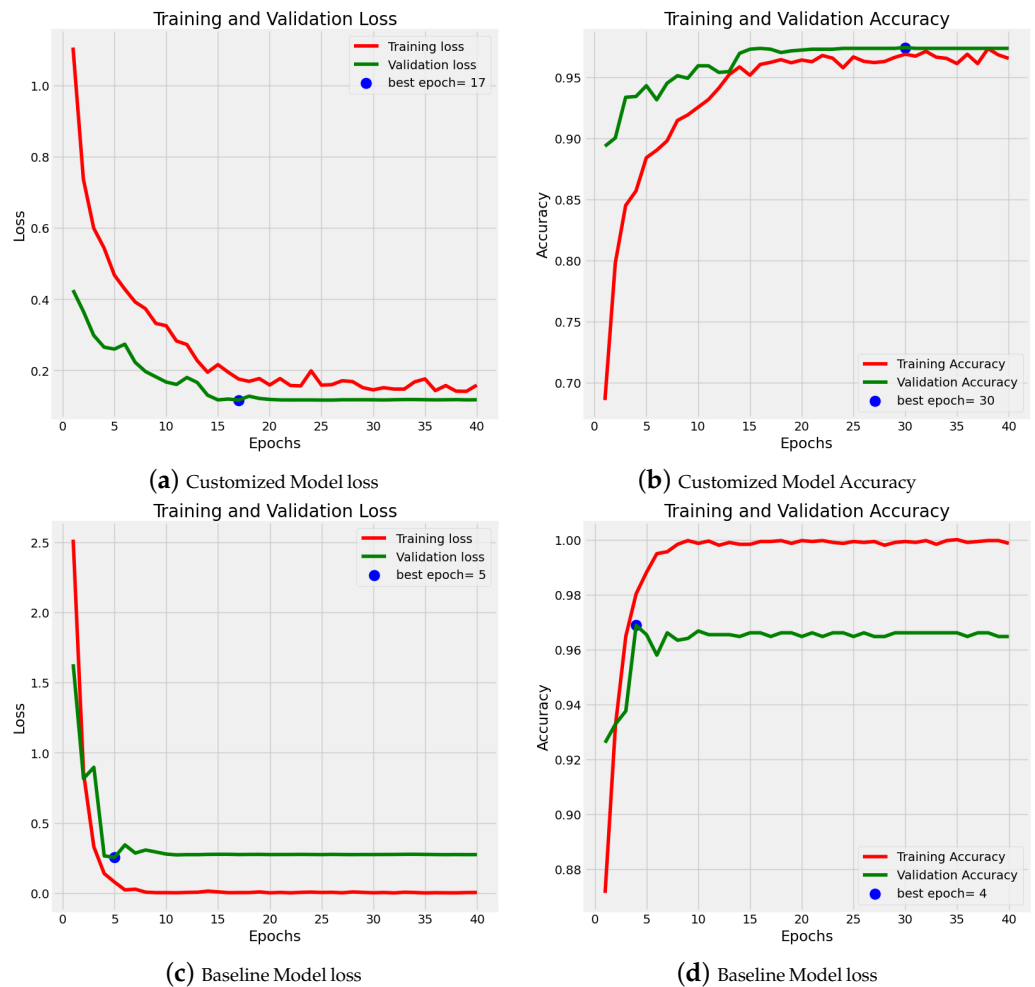
(**d**) Baseline Model loss

Figure 7. Accuracy and loss comparison between baseline and customized mode using Figshare dataset.

4.3. Performance Metric Comparison of the Proposed and State-of-the-Art Methods

As part of this research, an investigation was conducted to assess the model's robustness, including its parameter utilization across different architectures. The experimental results demonstrate in Table 4 show the effectiveness of our optimized EfficientNet im-

plementations. Our EfficientNetB1 achieves state-of-the-art accuracy of 98.6% with only 3.16 M parameters, representing a significant improvement over larger models like the Ensemble Model (147.74 M parameters, 96.9% accuracy) and Inception-ResnetV2 (73.9 M parameters, 93.8% accuracy). While MobileNetv3 reaches comparable accuracy (98.5%), our implementation maintains consistent performance above 98% across all variants with substantially fewer parameters—ranging from EfficientNetB0 (3.03 M) to B7 (8.37 M). This marks a notable improvement over the EfficientNet variants reported by [36], which required 5.9 M and 12.9 M parameters to achieve lower accuracies of 96.6% and 97.5% for B0 and B3, respectively.

Table 4. Comprehensive comparison of the obtained and previous studies results.

Variant	Params (M)	Acc (%)
EfficientNetB0 [36]	5.9	96.6
EfficientNetB3 [36]	12.9	97.5
Ensemble Model [37]	147.74	96.9
Inception-ResnetV2 [37]	73.9	93.8
MobileNetv3 [38]	–	98.5
CLAHE+CNN [39]	1.70	83.0
EfficientNetB0	3.03	98.5
EfficientNetB1	3.16	98.6
EfficientNetB2	3.59	98.3
EfficientNetB3	4.04	98.0
EfficientNetB4	4.99	98.0
EfficientNetB5	6.04	97.9
EfficientNetB6	7.16	98.0
EfficientNetB7	8.37	98.4

Table 4 demonstrates that the model's accuracy diminishes with an increase in the number of parameters. The fact that accuracy decreases as model size increases is in line with the fact that transfer learning is hard for domain-specific tasks, as shown in the EfficientNet study [14], where scaling benefits diminish as datasets decrease. Our strategy uses strict regularization (Dropout 0.5 + BatchNorm) to avoid medical imaging overfitting, which happens with insufficient training data and risks getting worse with larger models. The smallest models (B0-B2) find the best balance between regularization and reusing features. On the other hand, the classifier's static 32-unit bottleneck and large dropout make it too hard for the largest models (B3–B7) to use more parameters. This method is a compromise between two strategies: it prioritizes generalization (98.4% peak accuracy) over unrestricted scaling since adding too many parameters leads to small improvements at the cost of high computing power. The partial recovery at B7 signifies a continued capacity to overcome constraints, demonstrating EfficientNet's inherent resilience. Our methodology prioritizes domain-specific reliability, avoiding the limitations of basic scaling in biological applications.

In comparison to other architectures, our model places a higher emphasis on computational efficiency, which allows it to achieve equivalent diagnostic accuracy while utilizing a substantially smaller number of parameters, as illustrated in Table 4. Because of this streamlined design, training is completed more quickly, inference latency is reduced, making it suited for real-time applications, and the memory footprint is reduced. This makes it possible to deploy the model on devices with limited resources. Furthermore, our method makes complex diagnostic tools more accessible to a wider audience, which is especially beneficial in environments with limited resources.

4.4. Explainable AI (XAI) Interpretation and Further Assessment of the Method

To better understand the predictions of the deep model, we used gradient-weighted class activation mapping (Grad-CAM), a widely adopted XAI technique. Grad-CAM generates visual explanations by leveraging gradient information flowing into the final convolutional layer of the deep learning model. These gradients are globally averaged to produce weights for each feature map, which are then combined to create a coarse localization heatmap. This heatmap highlights regions of the input MRI scan that most strongly influenced the model's classification decision. This interpretation increased confidence among physicians, ensuring that the model's decisions were consistent with clinical expectations and knowledge.

Figure 8 demonstrates how artificial intelligence interprets different tumors through MRI visualization, presenting four key diagnostic categories—meningioma, glioma, pituitary, and non-tumor. Each category is displayed through original MRI sequences and their corresponding heat map activations, where warmer colors indicate areas of heightened diagnostic significance. Through enhanced preprocessing and activation mapping, the model provides clear identification of tumor-specific features, offering an intuitive yet technically robust approach to AI-assisted neuro-oncological classification.

Our detailed performance analysis compares both the baseline and customized models across the BT-3264 and BT-7023 datasets. Table 5 summarizes the findings across precision, recall, area under curve (AUC), and F1 Score. The customized model consistently outperforms the baseline model, with its additional layers significantly improving classification performance. The higher AUC values for the customized model demonstrate its enhanced ability to distinguish between different classes, reducing misclassification risk in clinical settings. Both models show improved performance with the larger BT-7023 dataset, indicating a positive correlation between dataset size and classification accuracy. However, the baseline model may face challenges in generalizing to unseen images. The analysis confirms our customized model's superior classification performance across both datasets, highlighting the importance of model adjustments and dataset size in medical image classification tasks.
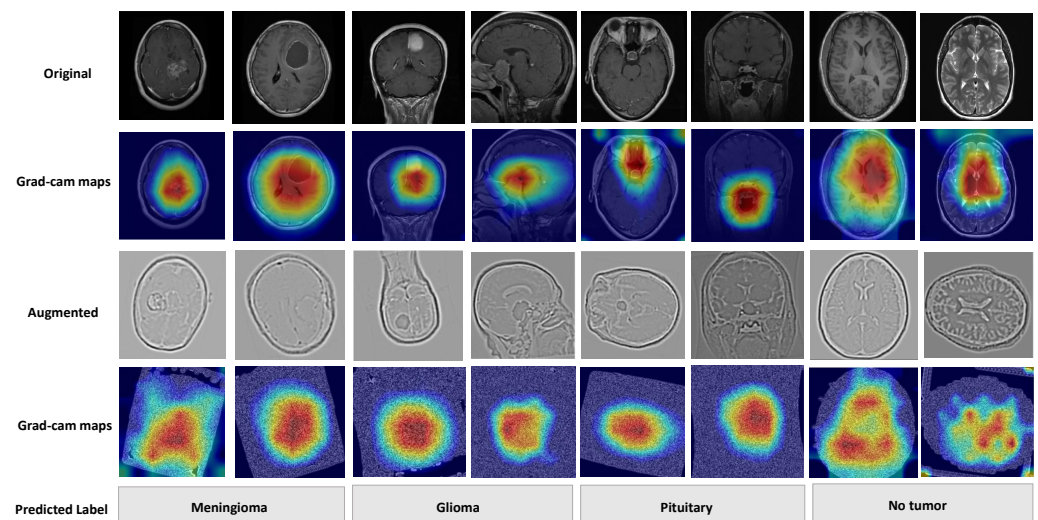

Figure 8. Visualization of different tumor types, showing the heat-maps for the original and augmented images (with labels). Each row displays the original MRI scan, the corresponding heatmap visualization, the augmented MRI scan with increased contrast and brightness, and the heatmap of the augmented image. Input image sample taken from the BT-3264 dataset [17].

Table 5. Precision, recall, AUC, and F1 score results of baseline vs. customized model.

Dataset	Model Type	Precision	Recall	AUC	F1 Score
BT_3264	Baseline	90	90	94	89
BT_3264	Customized	92	90	98	91
BT_7023	Baseline	96	96	97	96
BT_7023	Customized	97	97	99	97

5. Conclusions

Our research has demonstrated the potential of advanced deep learning techniques in revolutionizing brain tumor detection and classification. By refining the EfficientNet architecture, we developed a model that achieves high accuracy in distinguishing between glioma, meningioma, pituitary tumors, and normal brain tissue. This model's reduced number of parameters leads to lower computational resource requirements, while its enhanced interpretability is demonstrated through Grad-CAM visualization. This combination of performance and explainability addresses a critical need in medical AI applications. Our model demonstrates superior performance over existing state-of-the-art methods, achieving a 97.8% accuracy rate and 96.5% F1 score, underscoring the value of transfer learning and targeted architectural modifications in adapting general-purpose models to specialized medical tasks. The model's robustness, even with limited training data, suggests its potential for real-world clinical applications where large, diverse datasets may not always be available. While our current work focuses on MRI image analysis, we recognize the multifaceted nature of medical diagnosis. The integration of additional data modalities, such as patient history and genetic information, represents a promising direction for future research. This multi-modal approach could further enhance the model's diagnostic capabilities, potentially leading to more comprehensive and accurate tumor assessments.

6. Limitation and Future Work

Although our model performs well in classifying brain tumors, we must acknowledge several limitations. First, the fact that it only uses MRI data makes it harder to add more clinical information, like a patient's history, genetic markers, or results from other diagnostic tests. This limitation may reduce its effectiveness in handling rare tumor subtypes or under-represented patient populations. Additionally, our neural network is not inherently generalizable to different imaging modalities without adaptation or retraining. It was trained on MRI scans only, so how well it works on other imaging methods, like PET scans or functional MRI, is still unknown and would need more domain-specific adjustments. Furthermore, the proposed approach should work in conjunction with laboratory clinicians to execute the final diagnosis using the classification results from the model. This helps to alleviate any mistakes from AI-based models.

Future work should focus on developing multi-modal systems that combine imaging data with electronic health records and genomic information to enhance diagnostic accuracy and clinical relevance. Also, making models more flexible by using domain adaptation techniques or transfer learning could make them more useful for a wider range of medical imaging sources.

References

1. Seer. *Cancer Stat Facts: Brain and Other Nervous System Cancer*. Available online: https://seer.cancer.gov/statfacts/html/brain.html (accessed on 2 January 2025).

2. Sung, H.; Ferlay, J.; Siegel, R.L.; Laversanne, M.; Soerjomataram, I.; Jemal, A.; Bray, F. Global cancer statistics 2020: GLOBOCAN estimates of incidence and mortality worldwide for 36 cancers in 185 countries. *CA Cancer J. Clin.* **2021**, *71*, 209–249. [CrossRef]

3. Batool, A.; Byun, Y.C. Brain tumor detection with integrating traditional and computational intelligence approaches across diverse imaging modalities-Challenges and future directions. *Comput. Biol. Med.* **2024**, *175*, 108412. [CrossRef]

4. Sufyan, M.; Shokat, Z.; Ashfaq, U.A. Artificial intelligence in cancer diagnosis and therapy: Current status and future perspective. *Comput. Biol. Med.* **2023**, *165*, 107356. [CrossRef] [PubMed]

5. Gonzalez-Cava, J.M.; Arnay, R.; León, A.; Martín, M.; Reboso, J.A.; Calvo-Rolle, J.L.; Mendez-Perez, J.A. Machine learning based method for the evaluation of the Analgesia Nociception Index in the assessment of general anesthesia. *Comput. Biol. Med.* **2020**, *118*, 103645. [CrossRef] [PubMed]

6. Pascual, J.S.G.; de Lotbiniere-Bassett, M.; Khu, K.J.O.; Starreveld, Y.P.; Lama, S.; Legaspi, G.D.; Berger, M.S.; Duffau, H.; Sutherland, G.R. Challenges and Opportunities in Awake Craniotomy for Brain Tumor Surgery in Low- and Lower-Middle-Income Countries: A Narrative Review and Perspective. *World Neurosurg.* **2024**, *189*, 118–126. [CrossRef]

7. Raghavendra, U.; Gudigar, A.; Paul, A.; Goutham, T.; Inamdar, M.A.; Hegde, A.; Devi, A.; Ooi, C.P.; Deo, R.C.; Barua, P.D.; et al. Brain tumor detection and screening using artificial intelligence techniques: Current trends and future perspectives. *Comput. Biol. Med.* **2023**, *163*, 107063. [CrossRef] [PubMed]

8. Hržić, F.; Tschauner, S.; Sorantin, E.; Štajduhar, I. XAOM: A method for automatic alignment and orientation of radiographs for computer-aided medical diagnosis. *Comput. Biol. Med.* **2021**, *132*, 104300. [CrossRef]

9. Chukwujindu, E.; Faiz, H.; AI-Douri, S.; Faiz, K.; De Sequeira, A. Role of artificial intelligence in brain tumour imaging. *Eur. J. Radiol.* **2024**, *176*, 111509. [CrossRef]

10. Arabahmadi, M.; Farahbakhsh, R.; Rezazadeh, J. Deep learning for smart Healthcare—A survey on brain tumor detection from medical imaging. *Sensors* **2022**, *22*, 1960. [CrossRef] [PubMed]

11. Zhu, Z.; He, X.; Qi, G.; Li, Y.; Cong, B.; Liu, Y. Brain tumor segmentation based on the fusion of deep semantics and edge information in multimodal MRI. *Inf. Fusion* **2023**, *91*, 376–387. [CrossRef]

12. Liu, Y.; Shi, Y.; Mu, F.; Cheng, J.; Chen, X. Glioma Segmentation-Oriented Multi-Modal MR Image Fusion With Adversarial Learning. *IEEE/CAA J. Autom. Sin.* **2022**, *9*, 1528–1531. [CrossRef]

13. Zulfiqar, F.; Bajwa, U.I.; Mehmood, Y. Multi-class classification of brain tumor types from MR images using EfficientNets. *Biomed. Signal Process. Control* **2023**, *84*, 104777. [CrossRef]

14. Tan, M.; Le, Q. Efficientnet: Rethinking model scaling for convolutional neural networks. In Proceedings of the International Conference on Machine Learning. PMLR, pp. 6105–6114. Available online: http://proceedings.mlr.press/v97/tan19a.html?ref=jina-ai-gmbh.ghost.io (accessed on 2 January 2025).

15. Rehman, A.; Naz, S.; Razzak, M.I.; Akram, F.; Imran, M. A deep learning-based framework for automatic brain tumors classification using transfer learning. *Circuits Syst. Signal Process.* **2020**, *39*, 757–775. [CrossRef]

16. Cubuk, E.D.; Dyer, E.S.; Lopes, R.G.; Smullin, S. Tradeoffs in Data Augmentation: An Empirical Study. In Proceedings of the ICLR, Vienna, Austria, 4 May 2021. Available online: https://research.google/pubs/tradeoffs-in-data-augmentation-an-empirical-study/ (accessed on 2 January 2025).

17. Bhuvaji, S.; Kadam, A.; Bhumkar, P.; Dedge, S.; Kanchan, S. Brain Tumor Classification (MRI). 2020. Available online: https://www.kaggle.com/datasets/sartajbhuvaji/brain-tumor-classification-mri (accessed on 2 January 2025).

18. Nickparvar, M. Brain Tumor MRI Dataset. 2021. Available online: https://www.kaggle.com/datasets/masoudnickparvar/brain-tumor-mri-dataset. (accessed on 2 January 2025).

19. Rajini, N.H.; Bhavani, R. Classification of MRI brain images using k-nearest neighbor and artificial neural network. In Proceedings of the 2011 International Conference on Recent Trends in Information Technology (ICRTIT), Chennai, India, 3–5 June 2011; pp. 563–568. [CrossRef]

20. Yousef, R.; Gupta, G.; Yousef, N.; Khari, M. A holistic overview of deep learning approach in medical imaging. *Multimed. Syst.* **2022**, *28*, 881–914. [CrossRef]

21. Arbane, M.; Benlamri, R.; Brik, Y.; Djerioui, M. Transfer learning for automatic brain tumor classification using MRI images. In Proceedings of the 2020 2nd International Workshop on Human-Centric Smart Environments for Health and Well-being (IHSH), Boumerdes, Algeria, 9–10 February 2021; pp. 210–214. [CrossRef]

22. He, K.; Zhang, X.; Ren, S.; Sun, J. Deep Residual Learning for Image Recognition. In Proceedings of the 2016 IEEE Conference on Computer Vision and Pattern Recognition (CVPR), Las Vegas, NV, USA, 27–30 June 2016; pp. 770–778. [CrossRef]

23. Szegedy, C.; Liu, W.; Jia, Y.; Sermanet, P.; Reed, S.; Anguelov, D.; Erhan, D.; Vanhoucke, V.; Rabinovich, A. Going Deeper with Convolutions. *arXiv* **2014**, arXiv:1409.4842. [CrossRef]

24. Sandler, M.; Howard, A.G.; Zhu, M.; Zhmoginov, A.; Chen, L.C. MobileNetV2: Inverted Residuals and Linear Bottlenecks. In Proceedings of the 2018 IEEE/CVF Conference on Computer Vision and Pattern Recognition, Salt Lake City, UT, USA, 18–23 June 2018; pp. 4510–4520. Available online: https://openaccess.thecvf.com/content_cvpr_2018/html/Sandler_MobileNetV2_Inverted_Residuals_CVPR_2018_paper.html (accessed on 2 January 2025).

25. Amin, J.; Sharif, M.; Haldorai, A.; Yasmin, M.; Nayak, R.S. Brain tumor detection and classification using machine learning: A comprehensive survey. *Complex Intell. Syst.* **2022**, *8*, 3161–3183. [CrossRef]

26. Javaid, I.; Zhang, S.; Abd El Kader, I.; Kamhi, S.; Ahmad, I.; Kulsum, U. Brain Tumor Classification & Segmentation by Using Advanced DNN, CNN & ResNet-50 Neural Networks. *Int. J. Circuits, Syst. Signal Process.* **2020**, *14*, 1011–1029. [CrossRef]

27. Liu, S.; Deng, W. Very deep convolutional neural network based image classification using small training sample size. In Proceedings of the 2015 3rd IAPR Asian Conference on Pattern Recognition (ACPR), Kuala Lumpur, Malaysia, 3–6 November 2015; pp. 730–734. [CrossRef]

28. Shah, H.A.; Saeed, F.; Yun, S.; Park, J.H.; Paul, A.; Kang, J.M. A robust approach for brain tumor detection in magnetic resonance images using finetuned efficientnet. *IEEE Access* **2022**, *10*, 65426–65438. [CrossRef]

29. Yazdan, S.A.; Ahmad, R.; Iqbal, N.; Rizwan, A.; Khan, A.N.; Kim, D.H. An efficient multi-scale convolutional neural network based multi-class brain MRI classification for SaMD. *Tomography* **2022**, *8*, 1905–1927. [CrossRef]

30. Sajjad, M.; Khan, S.; Muhammad, K.; Wu, W.; Ullah, A.; Baik, S.W. Multi-grade brain tumor classification using deep CNN with extensive data augmentation. *J. Comput. Sci.* **2019**, *30*, 174–182. [CrossRef]

31. Dosovitskiy, A. An image is worth 16x16 words: Transformers for image recognition at scale. *arXiv* **2020**, arXiv:2010.11929. [CrossRef]

32. Shamshad, F.; Khan, S.; Zamir, S.W.; Khan, M.H.; Hayat, M.; Khan, F.S.; Fu, H. Transformers in medical imaging: A survey. *Med. Image Anal.* **2023**, *88*, 102802. [CrossRef]

33. Chen, C.Y.; Wu, K.H.; Guo, B.C.; Lin, W.Y.; Chang, Y.J.; Wei, C.W.; Lin, M.J.; Wu, H.P. Personalized medicine in severe asthma: From biomarkers to biologics. *Int. J. Mol. Sci.* **2023**, *25*, 182. [CrossRef]

34. Keras, Keras 3 API documentation. Available online: https://keras.io/guides/ (accessed on 1 January 2025).

35. Cheng, J. Brain Tumor Dataset, 2017. Available online: https://figshare.com/articles/dataset/brain_tumor_dataset/1512427/8 (accessed on 2 January 2025).

36. Reyes, D.; Sánchez, J. Performance of convolutional neural networks for the classification of brain tumors using magnetic resonance imaging. *Heliyon* **2024**, *10*, e25468. Available online: https://www.cell.com/heliyon/fulltext/S2405-8440(24)01499-3 (accessed on 2 January 2025). [CrossRef] [PubMed]

37. Hossain, S.; Chakrabarty, A.; Gadekallu, T.R.; Alazab, M.; Piran, M.J. Vision Transformers, Ensemble Model, and Transfer Learning Leveraging Explainable AI for Brain Tumor Detection and Classification. *IEEE J. Biomed. Health Informatics* **2024**, *28*, 1261–1272. [CrossRef]

38. Mathivanan, S.K.; Sonaimuthu, S.; Murugesan, S.; Rajadurai, H.; Shivahare, B.D.; Shah, M.A. Employing deep learning and transfer learning for accurate brain tumor detection. *Sci. Rep.* **2024**, *14*, 7232. [CrossRef] [PubMed]
39. Rasheed, Z.; Ma, Y.K.; Ullah, I.; Ghadi, Y.Y.; Khan, M.Z.; Khan, M.A.; Abdusalomov, A.; Alqahtani, F.; Shehata, A.M. Brain Tumor Classification from MRI Using Image Enhancement and Convolutional Neural Network Techniques. *Brain Sci.* **2023**, *13*, 1320. [CrossRef]